Lecture Notes in Computational Vision and Biomechanics 11

M. Emre Celebi
Bogdan Smolka *Editors*

Advances in Low-Level Color Image Processing

Springer

Lecture Notes in Computational Vision and Biomechanics

Volume 11

For further volumes:
http://www.springer.com/series/8910

The research related to the analysis of living structures (Biomechanics) has been a source of recent research in several distinct areas of science, for example, Mathematics, Mechanical Engineering, Physics, Informatics, Medicine and Sport. However, for its successful achievement, numerous research topics should be considered, such as image processing and analysis, geometric and numerical modelling, biomechanics, experimental analysis, mechanobiology and enhanced visualization, and their application to real cases must be developed and more investigation is needed. Additionally, enhanced hardware solutions and less invasive devices are demanded.

On the other hand, Image Analysis (Computational Vision) is used for the extraction of high level information from static images or dynamic image sequences. Examples of applications involving image analysis can be the study of motion of structures from image sequences, shape reconstruction from images and medical diagnosis. As a multidisciplinary area, Computational Vision considers techniques and methods from other disciplines, such as Artificial Intelligence, Signal Processing, Mathematics, Physics and Informatics. Despite the many research projects in this area, more robust and efficient methods of Computational Imaging are still demanded in many application domains in Medicine, and their validation in real scenarios is matter of urgency.

These two important and predominant branches of Science are increasingly considered to be strongly connected and related. Hence, the main goal of the LNCV&B book series consists of the provision of a comprehensive forum for discussion on the current state-of-the-art in these fields by emphasizing their connection. The book series covers (but is not limited to):

- Applications of Computational Vision and Biomechanics
- Biometrics and Biomedical Pattern Analysis
- Cellular Imaging and Cellular Mechanics
- Clinical Biomechanics
- Computational Bioimaging and Visualization
- Computational Biology in Biomedical Imaging
- Development of Biomechanical Devices
- Device and Technique Development for Biomedical Imaging
- Experimental Biomechanics
- Gait & Posture Mechanics
- Grid and High Performance Computing for Computational Vision and Biomechanics
- Image Processing and Analysis
- Image Processing and Visualization in Biofluids
- Image Understanding
- Material Models
- Mechanobiology
- Medical Image Analysis
- Molecular Mechanics
- Multi-Modal Image Systems
- Multiscale Biosensors in Biomedical Imaging
- Multiscale Devices and Biomems for Biomedical Imaging
- Musculoskeletal Biomechanics
- Multiscale Analysis in Biomechanics
- Neuromuscular Biomechanics
- Numerical Methods for Living Tissues
- Numerical Simulation
- Software Development on Computational Vision and Biomechanics
- Sport Biomechanics
- Virtual Reality in Biomechanics
- Vision Systems

M. Emre Celebi · Bogdan Smolka
Editors

Advances in Low-Level Color Image Processing

Springer

Editors
M. Emre Celebi
Computer Science Department
Louisiana State University
Shreveport, LA
USA

Bogdan Smolka
Department of Automatic Control
Silesian University of Technology
Gliwice
Poland

ISSN 2212-9391 ISSN 2212-9413 (electronic)
ISBN 978-94-007-7583-1 ISBN 978-94-007-7584-8 (eBook)
DOI 10.1007/978-94-007-7584-8
Springer Dordrecht Heidelberg New York London

Library of Congress Control Number: 2013953224

Printed on acid-free paper

Springer is part of Springer Science+Business Media (www.springer.com)

Preface

Color perception plays an important role in object recognition and scene understanding both for humans and intelligent vision systems. Recent advances in digital color imaging and computer hardware technology have led to an explosion in the use of color images in a variety of applications including medical imaging, content-based image retrieval, biometrics, watermarking, digital inpainting, remote sensing, visual quality inspection, among many others. As a result, automated processing and analysis of color images has become an active area of research, which is witnessed by the large number of publications during the past two decades. The multivariate nature of color image data presents new challenges for researchers and practitioners as the numerous methods developed for single channel images are often not directly applicable to multichannel ones.

The goal of this volume is to summarize the state-of-the-art in the early stages of the color image processing pipeline. The intended audience includes researchers and practitioners, who are increasingly using color and, in general, multichannel images.

The volume opens with two chapters on image acquisition. In Chap. 1 Chen et al. focus on the problem of color artifacts generated by line-scan cameras. They propose a method that enables automated correction of the color misalignment in multi-line CCD images for rotational and translational scans. The chapter presents the experimental results achieved using a close-range multi-line CCD imaging system for inspection applications and a long-range camera intended for surveillance tasks. The results confirm that the two imaging systems enable the acquisition of hyper-resolution images with effective color misalignment adjustment.

In Chap. 2 Lee and Park propose a novel adaptive technique for color image demosaicking that exploits the characteristics of the CFA pattern. Comparative experiments performed on a large set of test images show the effectiveness of the proposed interpolation algorithm in terms of peak signal-to-noise ratio, structural similarity, and subjective visual quality. The new algorithm outperforms conventional algorithms especially in the case of natural images containing many image structures such as lines, edges, and corners.

The volume continues with two chapters on color constancy. In Chap. 3 Lee and Plataniotis et al. present a comprehensive survey of color constancy and color invariance. The color of an object recorded in image data is not only a function of an intrinsic property of the object itself, but also a function of the acquisition

device and the prevailing illumination. When these factors are not properly controlled, the performance of color image processing applications can deteriorate substantially. The Authors review two common approaches to attain reliable color description of image data under varying imaging conditions, namely, color constancy and color invariance, where the former is based on scene illuminant estimation and image correction, while the latter is based on invariant feature extraction.

In Chap. 4 Lecca describes applications of the von Kries model of chromatic adaptation to color correction, illuminant invariant image retrieval, estimation of color temperature and intensity of light, and photometric characterization of a device. The von Kries model describes the change in image colors due to illuminant variation. Lecca first illustrates the theoretical foundations of the von Kries model. The Author then presents a method for the model parameter estimation and derives a mathematical relationship between the parameters of the von Kries model and the color temperatures and intensities of the varied illuminants. The chapter concludes by showing a model relating the von Kries parameters to the photometric properties of the acquisition device. Through this model, it is possible to estimate the light wavelengths for which the camera sensors are maximally responsive. These wavelengths are used for finding an illuminant invariant image representation. The chapter reports various experiments carried out on publicly available real-world datasets.

In Chap. 5 Baljozovic et al. propose a novel algorithm for removing impulsive or mixed noise from color images based on the halfspace depth function. The resulting multichannel filter maintains the spectral correlation between the color channels and does not depend on the nature or distribution of the noise. The Authors compare the performance of their filter against a large number of state-of-the-art noise removal filters on a diverse set of images.

The volume continues with three chapters on mathematical morphology. In Chap. 6 Debayle and Pinoli present a spatially adaptive image processing framework based on the General Adaptive Neighborhood Image Processing (GANIP) concept. The Authors extend the GANIP approach to color images and define a set of locally adaptive image processing operators. Special emphasis is given to adaptive fuzzy and morphological filters, which are compared to their classic counterparts in restoration, enhancement, and segmentation of color images.

In Chap. 7 Velasco and Angulo investigate the applicability of recent multivariate ordering approaches to morphological analysis of color and multispectral images. The Authors survey supervised learning and anomaly based ordering approaches and present applications of each.

In Chap. 8 Lefèvre et al. review morphological template matching using the Hit-or-Miss Transform (HMT) operator. The Authors review the application of HMT to binary, grayscale, and color images. They also discuss several case studies illustrating practical applications of HMT in different application domains.

The volume continues with two chapters on segmentation. In Chap. 9 Moreno et al. propose two powerful color edge detection methods based on the tensor

voting concept, which extracts structures from a cloud of multidimensional points. The proposed edge detection techniques are evaluated based on measures of completeness, discriminability, precision, and robustness to noise. Experimental results on a database with ground-truth edges reveal useful properties of the new methods, especially in the case of color images distorted by a Gaussian noise process.

In Chap. 10 Alarcon and Dalmau first review various discrete and fuzzy-based color categorization models and then they focus on a new framework which provides a probabilistic partition of a given color space. The proposed approach combines the color categorization model with a probabilistic segmentation algorithm and generalizes it including the interaction between categories. The effectiveness of the proposed approach is illustrated using various applications including color image segmentation, edge detection, video re-colorization, and object tracking.

In Chap. 11 Kawulok et al. present an overview of skin detection. The Authors focus on approaches based on pixel classification and present a comparative study of various state-of-the-art methods. They give an overview of techniques which model the skin color using a set of fixed rules, as well as those based on machine learning. In the latter case, the Authors report an experimental study which shows the sensitivity of commonly used methods to the number of samples in the training set. Not only are the techniques for skin color modeling explored, but also important approaches toward reducing skin detection errors are presented and validated empirically. In particular, the Authors outline the possibilities of adapting the skin color models to specific lighting conditions or to an individual, whose skin regions are to be segmented. In addition, the Authors present how the textural features and spatial analysis of the skin probability maps can be employed for skin detection.

In Chap. 12 Lee et al. address the issues connected with the employment of skin color as a feature in automatic face detection systems. After providing a general overview of face detection methods utilizing color information, the Authors discuss approaches for modeling skin color distribution in various color spaces, focusing on the influence of illumination conditions on the skin detection results and describe practical applications of skin color classification in high-level image processing systems. The effectiveness of color cues in terms of detection performance and computational efficiency is addressed using two distinct case studies.

Chapter 13 by Jiang et al. completes the volume. The Authors describe a very interesting application of color-based visual saliency in the design of video games. They provide an overview of several state-of-the-art saliency estimation methods and propose novel methods which are evaluated and compared with previously published techniques on an image saliency dataset. The proposed saliency estimation frameworks are applied to the visual game design process. The results demonstrate that the incorporation of color saliency information improves the visual quality of the video games and substantially increases their attractiveness.

As Editors, we hope that this volume focused on low-level color image processing will demonstrate the significant progress that has occurred in this field in

recent years. We also hope that the developments reported in this volume will motivate further research in this exciting field.

M. Emre Celebi
Bogdan Smolka

Contents

Automated Color Misalignment Correction for Close-Range and Long-Range Hyper-Resolution Multi-Line CCD Images 1
Zhiyu Chen, Andreas Koschan, Chung-Hao Chen and Mongi Abidi

Adaptive Demosaicing Algorithm Using Characteristics of the Color Filter Array Pattern 29
Ji Won Lee and Rae-Hong Park

A Taxonomy of Color Constancy and Invariance Algorithm 55
Dohyoung Lee and Konstantinos N. Plataniotis

On the von Kries Model: Estimation, Dependence on Light and Device, and Applications 95
Michela Lecca

Impulse and Mixed Multichannel Denoising Using Statistical Halfspace Depth Functions 137
Djordje Baljozović, Aleksandra Baljozović and Branko Kovačević

Spatially Adaptive Color Image Processing 195
Johan Debayle and Jean-Charles Pinoli

Vector Ordering and Multispectral Morphological Image Processing 223
Santiago Velasco-Forero and Jesus Angulo

Morphological Template Matching in Color Images 241
Sébastien Lefèvre, Erchan Aptoula, Benjamin Perret and Jonathan Weber

Tensor Voting for Robust Color Edge Detection 279
Rodrigo Moreno, Miguel Angel Garcia and Domenec Puig

Color Categorization Models for Color Image Segmentation 303
Teresa Alarcon and Oscar Dalmau

Skin Detection and Segmentation in Color Images 329
Michal Kawulok, Jakub Nalepa and Jolanta Kawulok

Contribution of Skin Color Cue in Face Detection Applications 367
Dohyoung Lee, Jeaff Wang and Konstantinos N. Plataniotis

Color Saliency Evaluation for Video Game Design 409
Richard M. Jiang, Ahmed Bouridane and Abbes Amira

Erratum to: On the von Kries Model: Estimation, Dependence on Light and Device, and Applications E1
Michela Lecca

Erratum to: Skin Detection and Segmentation in Color Images E3
Michal Kawulok, Jakub Nalepa and Jolanta Kawulok

Automated Color Misalignment Correction for Close-Range and Long-Range Hyper-Resolution Multi-Line CCD Images

Zhiyu Chen, Andreas Koschan, Chung-Hao Chen and Mongi Abidi

Abstract Surveillance and inspection have an important role in security and industry applications and are often carried out with line-scan cameras. The advantages of line-scan cameras include hyper-resolution (larger than 50 Megapixels), continuous image generation, and low cost, to mention a few. However, due to the physical separation of line CCD sensors for the red (R), green (G), and blue (B) color channels, the color images acquired by multi-line CCD cameras intrinsically exhibit a color misalignment defect, such that the edges of objects in the scene are separated by a certain number of pixels in the R, G, B color planes in the scan direction. This defect, if not corrected properly, can severely degrade the quality of multi-line CCD images and hence impairs the functionality of the cameras. Current techniques for correcting such color misalignments are typically not fully automated, which is undesirable in applications such as inspection and surveillance that depend on fast unmanned responses. This chapter introduces an algorithm to automatically correct the color misalignments in multi-line CCD images for rotational scans as well as for translational scans. Results are presented for two different configurations of multi-line CCD imaging systems: (a) a close-range multi-line CCD imaging system for inspection applications and (b) a long-range imaging system for surveillance applications. Experimental results show that the two imaging systems are able to acquire hyper-resolution images and the color misalignment correction algorithm can automatically and accurately correct those images for their respective applications.

Z. Chen (✉)
Seagate Technology PLC, Bloomington, MN, USA

A. Koschan · M. Abidi
Imaging, Robotics, and Intelligent Systems Laboratory,
Department of Electrical Engineering and Computer Science,
The University of Tennessee, Knoxville, TN, USA

C.-H. Chen
Department of Electrical and Computer Engineering,
Old Dominion University, Norfolk, VA, USA

M. E. Celebi and B. Smolka (eds.), *Advances in Low-Level Color Image Processing*, Lecture Notes in Computational Vision and Biomechanics 11,
DOI: 10.1007/978-94-007-7584-8_1,

Keywords Color correction · Color misalignment · Hyper-resolution color image · Multi-line CCD camera · Line-scan camera · Image acquisition · Imaging system

1 Introduction

Remote sensing, surveillance and inspectional scanning have an important role in security and industry applications and usually require acquiring hyper-resolution (larger than 50 Megapixels) images of a constant stream of materials or landscapes with relative motion. Such applications are often carried out with line-scan cameras because of their advantages, including: (i) hyper-resolution (at least thousands of pixels in one dimension and the size in the other dimension is limited only by the capacity of storage device); (ii) continuous image generation (video stream compared to discrete video frames generated from a frame-based camera); (iii) low cost (compared to still image cameras with a 2-D imaging sensor array that can achieve the same resolution).

1.1 Line-Scan Imaging Sensor and Applications

A line-scan camera is an imaging device generally containing a line-scan imaging sensor chip, supporting electronics and an optical system that includes one or multiple lenses and a focusing mechanism. Gupta et al. introduced a simplified camera model for line-scan imaging sensors [1]. Unlike video cameras and regular still image cameras, a line-scan camera has a single row (1-D) of pixel sensors, instead of a 2-D array of them.

Figure 1a shows a picture of a line-scan camera without the lens and focusing mechanism. Figure 1b illustrates the configuration of the RGB-multi-line CCD sensor on that camera which is capable of capturing color images.

There are two major technologies for solid-state imaging sensors, i.e., CCD (Charge-Coupled Devices) sensors and CMOS (Complementary Metal Oxide Semiconductor) sensors. The charge-coupled device was invented in 1969 at AT&T Bell Laboratories by Willard Boyle and George E. Smith [2–5]. CCDs have been in existence for over four decades and the technology has matured to the point where very large, consistent devices can now be manufactured. Compared to CCD technology, the CMOS imaging sensor technology is not as mature, but it is set to develop rapidly and offer a number of advantages over CCDs in terms of low power, low cost and monolithic integration. Nowadays active pixel CMOS imaging sensors have been optimized for optical sensing and can rival CCD counterparts in most aspects [6, 7].

One image frame captured by a line-scan camera contains only one row of pixels. In order to capture a 2-D image with such a camera, the 1-D frames are continuously fed to a computer that joins them to each other. Due to the much shorter time of transferring 1-D frames instead of 2-D frames out of the imaging chip, line-scan

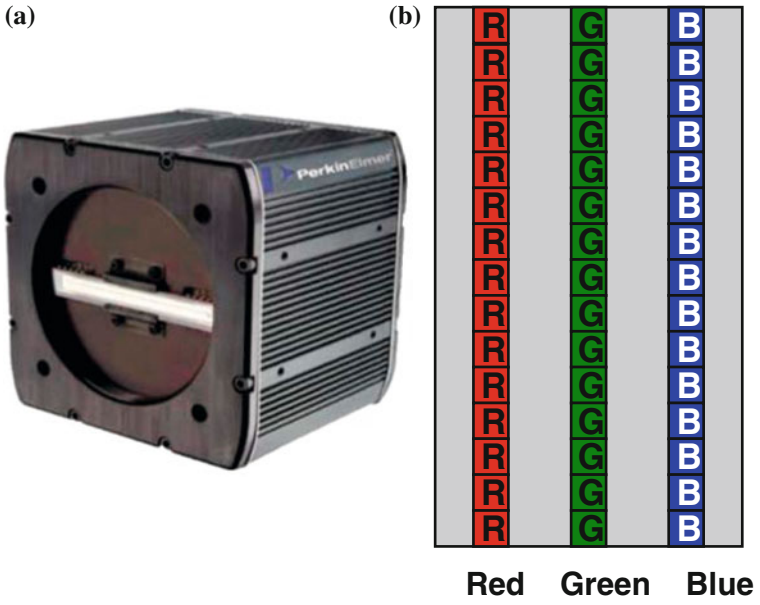

Fig. 1 **a** A line-scan CCD camera with three line sensors for color image capture. **b** Illustration of RGB line-scan sensors

cameras are capable of capturing sharp hyper-resolution images of objects passing in front of the camera at high speeds. Therefore, this kind of camera is commonly used in sports events to acquire photo finishes, i.e. to determine the winner when multiple competitors cross the finishing line at nearly the same time. Line-scan CCD cameras have significant advantages and play important roles in many industrial, scientific and military applications. The areas in which line-scan cameras have important applications include, but are not limited to, remote sensing, surveillance, high speed document/film scanning, industrial quality control inspection, surface inspection, racing sports, etc. Common applications of line-scan cameras in the area of remote sensing and surveillance include satellite and aerial imaging, and their applications in the area of industrial quality control inspection include printing inspection, produce and food inspection, textile inspection, etc.

Line-scan technology is capable of capturing data extremely fast and at very high image resolutions. Under such conditions the acquired image data can quickly exceed 100 MB in a matter of seconds. Data coming from the line-scan camera has a frequency at which the camera scans a line, waits, and repeats. The one-dimensional line data from the line-scan camera is commonly collected by image acquisition electronics, e.g., a frame grabber card in a computer, and then processed by the computer to create a 2-D image. The raw 2-D image is then processed by image-processing techniques in order to meet application objectives. Figure 2 illustrates the data path of a line-scan imaging system.

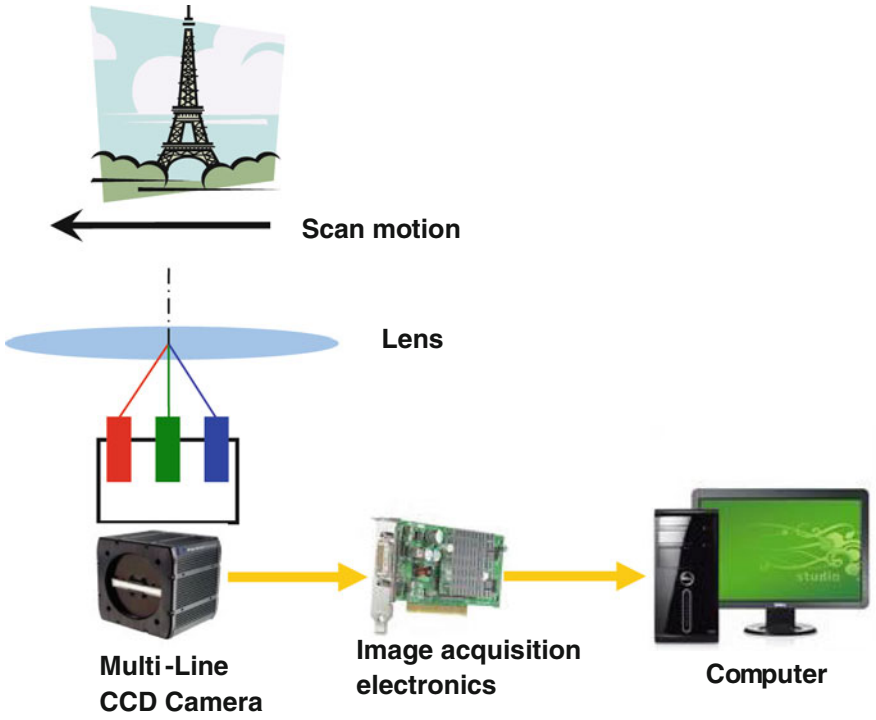

Fig. 2 The data path of a line-scan imaging system

Numerous novel applications of line-scan imaging systems have been reported in the literature. For example, Wilson reported an on-line surface inspection system designed to characterize the rotary screen-print process of applying up to 20 separate colors to a continuous textile web for the textile industry [8]. Reulke et al. developed a mapping method of combining high resolution images acquired by a line CCD camera with depth data acquired by a laser scanner. Application areas are city modeling, computer vision and documentation of cultural heritage [9–12]. Huang et al. developed a rotating-line-camera imaging system for stereo viewing and stereo reconstruction [13, 14]. Maresch et al. used three partially inclined and vertical linear CCD arrays and developed a vehicle-based 3-line CCD camera system for 3D city modeling [15]. Yoshioka et al. developed a vehicle lane change aid system (LCAS) with multi-line CCD sensors [16]. Bowden et al. designed a line-scanned micro Raman spectrometer using a cooled CCD imaging detector to obtain sequences of Raman spectra [17]. Ricny et al. developed an autonomous optoelectronic method of measuring the flying objects track velocity vector using two-line CCD sensors [18]. Kroll et al. developed a system using an 8-bit CCD line scanner for automatic determination of the brightness of star-like objects on a photographic plate [19]. Demircan et al. used a wide angle CCD line camera to measure the bi-directional reflectance distribution function of natural surfaces [20]. Kipman et al. developed a method of

measuring gloss mottle and micro-gloss using a line-scan CCD camera [21]. Rosen et al. used a line-scan CCD image sensor for on-line measurement of red blood cell velocity and microvascular diameter [22].

1.2 Color Misalignment Defect of Multi-Line CCD Images and its Correction

Hyper-resolution is one of the major advantages of line CCD images. However, due to the physical configuration and characteristics of multi-line CCD sensors, raw output images acquired by multi-line CCD cameras typically exhibit some defects, and may not be usable for desired application purposes. For example, because of the physical separation of line CCD sensors for the red (R), green (G), and blue (B) color channel, the color images acquired by multi-line CCD cameras intrinsically exhibit a color misalignment defect, such that the edges of objects in the scene are separated by a certain number of pixels in the R, G, B color planes in the scan direction. This defect, if not corrected properly, can severely degrade the quality of multi-line CCD images and hence impair the functionality of multi-line CCD cameras. Figure 3 illustrates the creation of color misalignment, and Fig. 4 shows a raw multi-line CCD image with such a defect. This misalignment can be considered a major problem in hyper-resolution multi-line CCD scans and is also called pixel lag [23] or video delay [24]. There are two commonly used methods for correcting color misalignment in multi-line CCD imaging:

(1) Synchronize the CCD line acquisition rate to the object's moving speed and/or the camera's scan motion [23].
(2) Set the video delay parameter of the multi-line CCD camera to compensate the target motion for the physical separation of color sensors. When the camera reconstructs the color image, the adjacent color planes are shifted by a certain number of lines that was specified by the video delay parameter [24].

The above methods have significant drawbacks and/or limitations. Both methods are not fully automated. Synchronizing the line acquisition rate to the object's motion is not an easy task. Furthermore, this method puts undesirable constraints on imaging parameters, e.g., line acquisition rate, exposure time, aspect ratio of acquired images, etc. The imaging parameters that synchronize the line acquisition rate to the scan motion speed may create images with undesirable or even unacceptable brightness and aspect ratios. Setting the video delay parameter can avoid putting undesirable constraints on imaging parameters; however, similar to the synchronization method, setting the correct video delay parameter before and/or when imaging is taking place is not an easy task. It is usually done by the user via visual inspection, which is subjective and not accurate, and the acquired images may still exhibit small color misalignment.

Since the current techniques for correcting color misalignments are not fully automated, and may put adverse constraints on imaging parameters, they are undesirable

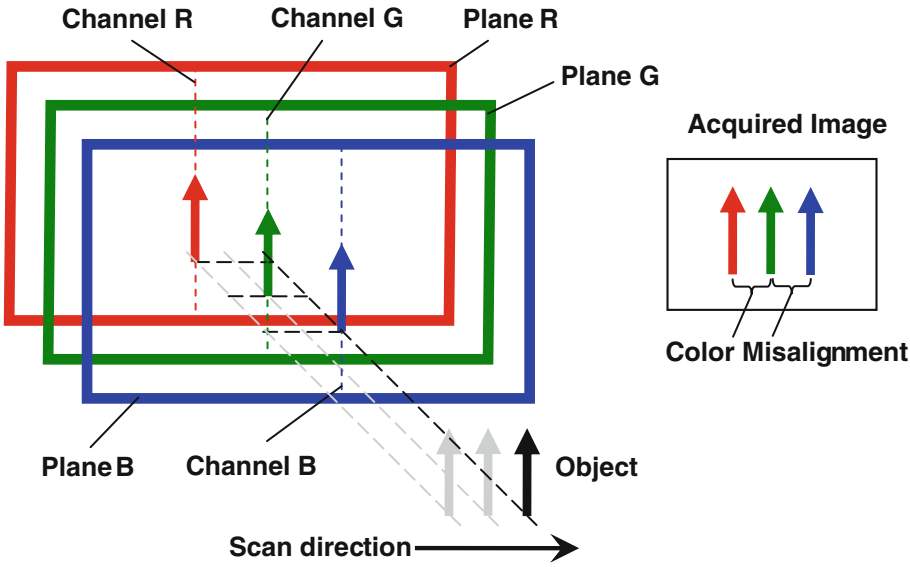

Fig. 3 Illustration of the creation of color misalignment

in applications such as inspection and surveillance that depend on fast unmanned responses. In order to greatly expand the applications of multi-line-scan cameras, it is important to develop a technique that can fully-automatically correct color misalignments in multi-line CCD images and does not put constraints on imaging parameters.

This chapter introduces an algorithm to automatically correct color misalignments in multi-line CCD images for rotational scans as well as for translational scans. Results are presented for two different configurations of multi-line CCD imaging systems: (a) a close-range multi-line CCD imaging system for inspection applications and (b) a long-range multi-line CCD imaging system for surveillance applications. This chapter is organized as follows: Section 2 presents the setup of two of our multi-line CCD imaging systems. Section 3 introduces a fully-automated color misalignment correction algorithm. Experimental results are presented in Sects. 4 and 5 concludes this chapter.

2 Multi-Line CCD Imaging Systems

We used a multi-line CCD camera to develop two hyper-resolution imaging systems, i.e., a close-range line-scan imaging system for inspection applications and a long-range system for surveillance applications. In the following, the configurations of the two imaging systems are presented.

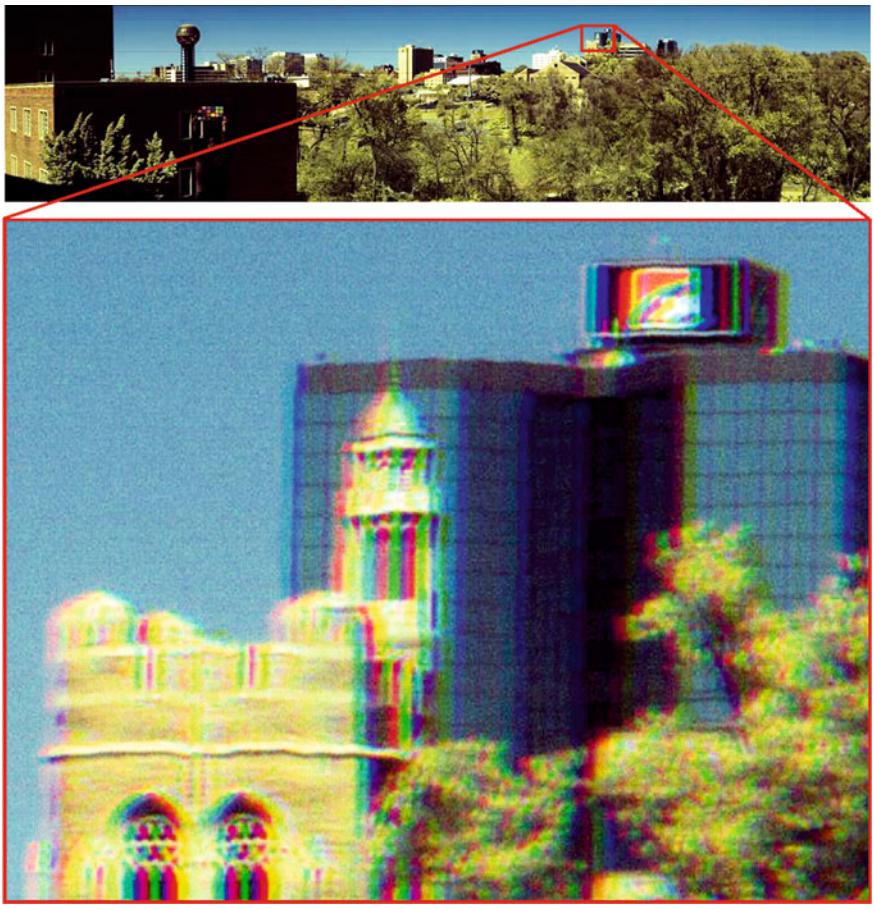

Fig. 4 Color misalignment in a multi-line CCD image

2.1 Translational Scan and Rotational Scan

In order to create 2-D images, a relative scan motion between the line-scan camera and the scene is necessary during the imaging process. There are two kinds of scan schemes—translational scan and rotational scan. Figures 5 and 6 illustrate two translational scan schemes. Translational scan is more suitable for close-range imaging; since the distance between the object to be imaged and the lens is constant in translational scan, the focus does not need to be adjusted and the image remains focused during the imaging process. For close range imaging, due to narrow depth of field, the object is usually a flat surface or an object with small depth. In the scan scheme illustrated in Fig. 5, the object is located on a platform which can undergo a translational scan motion across the field of view of the line-scan camera, and the scan

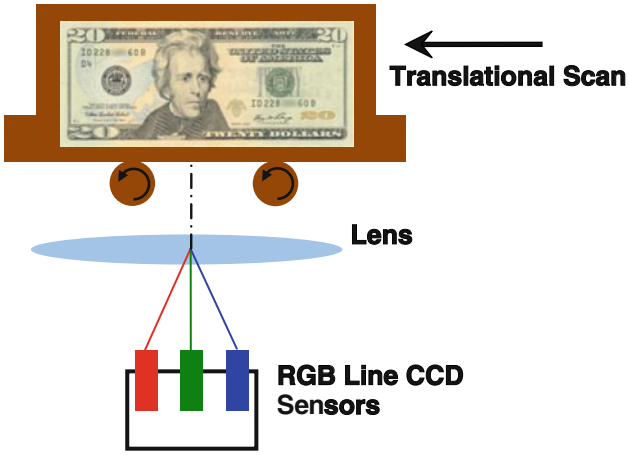

Fig. 5 A close-range imaging system with translational scan scheme

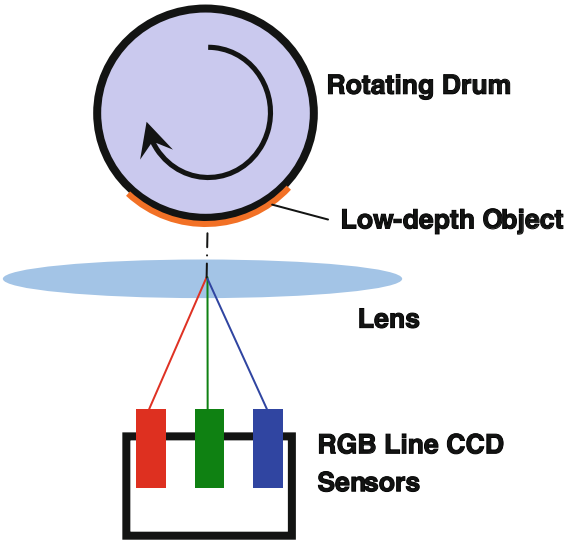

Fig. 6 A close-range imaging system with translational scan schem

speed can be adjusted by the user to change the aspect ratio of acquired images. In the scan scheme illustrated in Fig. 6, a rotating drum is placed in front of the camera lens to provide the scan motion. A flat or low-depth object is attached to the drum surface. Although the drum rotates, the scan motion seen by the line-scan camera is translational.

Figures 7 and 8 illustrate two rotational scan schemes. Rotational scan is more suitable for long-range imaging, since it enables the line-scan camera to scan a wide

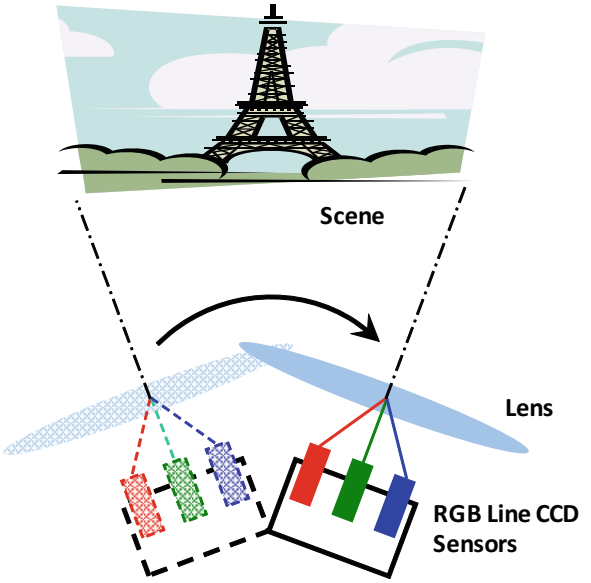

Fig. 7 A long-range imaging system with a rotating camera to provide scan motion

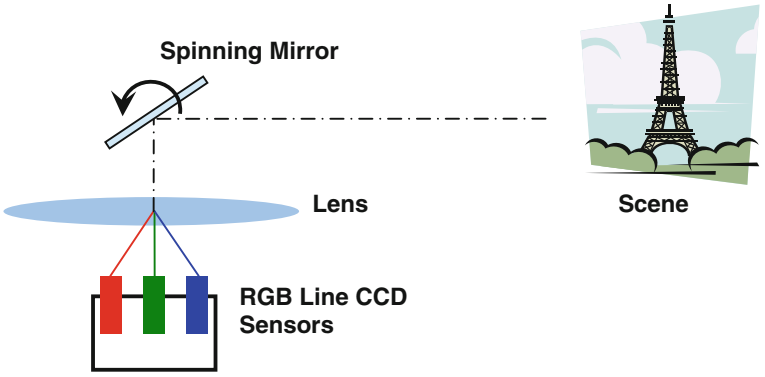

Fig. 8 A long-range imaging system with a rotating camera to provide scan motion

scene with the camera being fixed to one location. There are two ways to provide a rotational scan motion for a long-range imaging system:

(1) The camera rotates to sweep across the scene. Figure 7 shows the schematic of a long-range imaging system with a rotating camera to provide scan motion.
(2) A spinning mirror is placed in front of the camera lens and reflects the moving scene into camera. Figure 8 shows the schematic of a long-range imaging system with a spinning mirror to provide scan motion.

The spinning mirror design has a significant advantage over the rotating camera design, because the mechanical system for spinning a long, narrow light-weight mirror is smaller, lighter and less expensive than that for rotating the entire imaging system; therefore, the system is more mobile and more suitable for outdoor applications. The disadvantage of the spinning mirror design is that it is more susceptible to wind when used for outdoor image acquisitions because of the mirror's light weight and relatively large area. Wind can cause the mirror to vibrate slightly, and slight vibrations of the spinning mirror can severely impair the quality of acquired images because of the hyper-resolution nature of these images. Therefore, in order to minimize the effect of wind and mechanical vibration, the rotation mechanism and the fixture for attaching the mirror to the mechanism need to be carefully designed. In addition, the wind effect can be significantly reduced by placing a glass windshield in front of the spinning mirror.

2.2 Close-Range Multi-Line CCD Imaging System

We developed a close-range multi-line CCD imaging system incorporating a Perkin-Elmer multi-line-scan camera for inspection applications. A picture of this system is shown in Fig. 9. This imaging system consists of a YD5060 tri-linear CCD color camera, a bellows, a short focal-length (90 mm) lens, DC diffusive illumination lights, and scanning mechanism. These system components are mounted on a metal plate platform for stabilization and easy transportation. The DC diffusive lights provide intense, constant and uniform illumination over the object to ensure that the image formed on sensor lines has sufficient brightness.

The bellows connects to the camera and the lens at two ends. The bellows length is adjustable for changing focusing and magnification. For close-range inspection applications, our goal is to image a small area of interest (e.g., a few centimeters or smaller in one dimension) on the inspected surface with a hyper-resolution of 6,144 pixels in one dimension. Therefore, high magnification is required in order for the lens to create an image of the small area of interest at the camera sensor plane, and the image should have the same number of lines as there are CCD sensor lines. High magnification is achieved with a long bellows length ($\sim$60 cm) and a short distance ($\sim$10 cm) between the camera lens and the surface to be inspected. The optical magnification of this system is 6$\times$, resulting in that a pixel on the CCD sensor line corresponds to 1.5 μm on the object, and this 1.5 μm is close to the size limit of a feature that can be discerned by visible light because of diffraction limit. Therefore, this imaging system is capable of capturing an object's micron-scale fine details, and it has almost reached the size limit discernible by visible light. A microscope can achieve a similar scale; however, for microscopic imaging, the object to be imaged is often cut into thin slices or small pieces, and this destructive imaging method cannot be accepted for many applications such as weld inspection. Therefore, close-range line CCD imaging has an advantage over microscopic imaging for non-destructive inspection imaging applications. In addition, close-range line-scan imaging does not

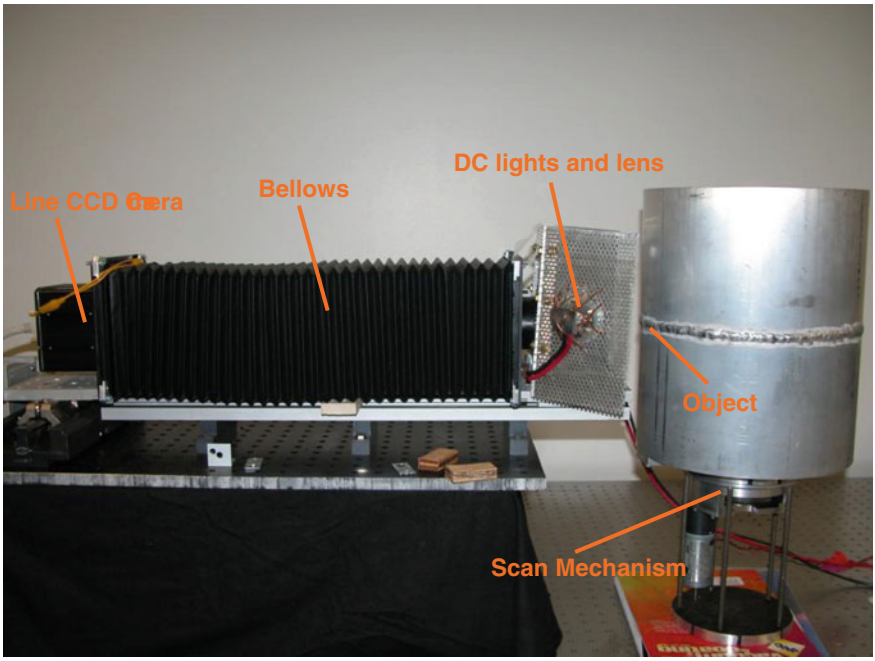

Fig. 9 Example of a close-range imaging system

put a limit on the object's length, and acquires images with higher resolution and faster speed.

Figure 10a illustrates the optical path of image formation for close-range imaging. The distances between the object and lens, and the lens and image plane, are related by the thin lens formula,

$$\frac{1}{d_o} + \frac{1}{d_i} = \frac{1}{f}, \tag{1}$$

where d_o is the distance from the object plane to the center of the lens, d_i is the distance from the image plane to the center of the lens, and f is the focal length of the lens. Since $d_o \gg d_i$, the size of the formed image is much larger than that of the object; it makes this close-range imaging system more suitable for surface inspection applications.

For close-range imaging applications, due to the high magnification and short exposure time (a few milliseconds) used in line-scan CCD imaging, intense illumination is required in order to acquire images with proper brightness.

In our system, two DC projector light bulbs are used to provide this illumination. The light bulbs are located on each side of the camera lens, pointing to the object that is imaged. DC power is necessary in order to provide time-invariant constant illumination for line scan imaging. At one end of the metal base platform there is a small translational scan platform, which is connected to a gear box and driven by a

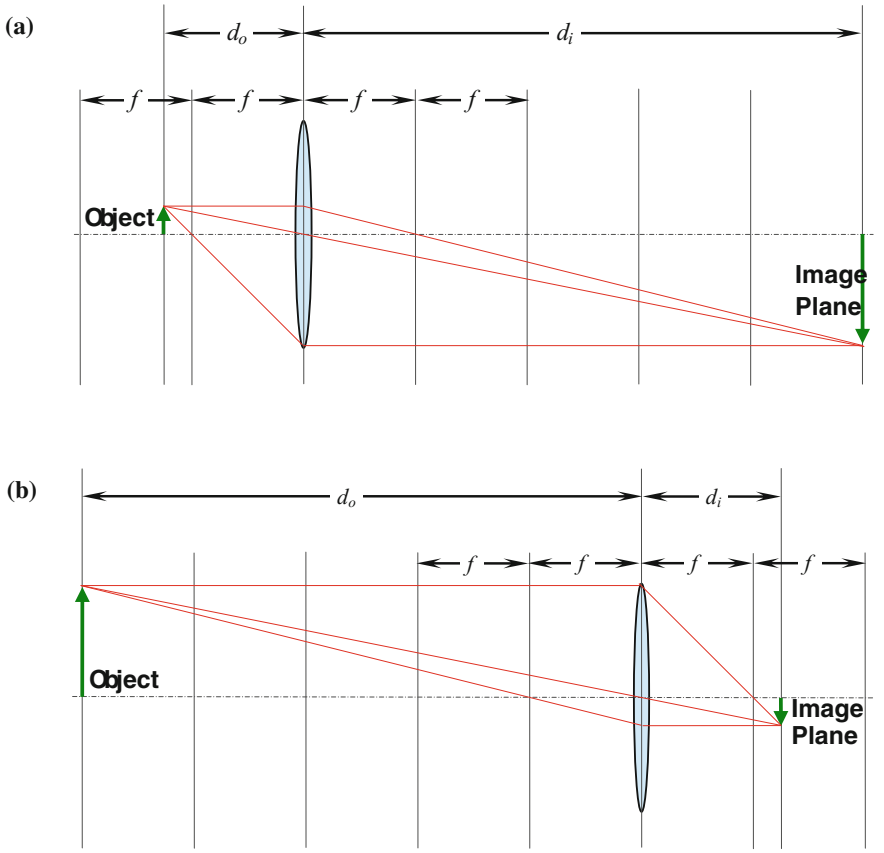

Fig. 10 Optics of multi-line CCD imaging systems: **a** Close-range system and **b** Long-range system

computerized stepping motor. The stepping motor is powered and controlled by an electronic control card, which is connected to a PC computer through a serial port. Therefore, the scan direction and speed can be controlled by the user through the computer.

In one of the close-range imaging configurations, the object to be imaged is positioned on the translational scan platform at one end of the base platform, and the multi-line-scan camera is located on the other end. When being imaged, the object moves with the translational scan platform in the direction perpendicular to the optical axis of the line-scan camera. In another close-range imaging setup, the object to be imaged is placed on a spinning drum which is positioned in front of the camera lens, as shown in Fig. 9. When the drum rotates, it moves the object attached to it and provides the translational scan motion for the line-scan camera to take an image. The spin speed of the drum can be adjusted by adjusting the voltage applied on the driving motor.

2.3 Long-Range Multi-Line CCD Imaging System

We also developed a long-range multi-line CCD imaging system incorporating the PerkinElmer YD5060 line-scan camera for surveillance and security monitoring applications. A picture of this system is shown in Fig. 11. This imaging system consists of a tri-linear CCD color camera, a bellows, a long focal-length (508 mm) lens, and a geared spinning mirror mechanism for providing rotational scan motion. These system components are mounted on a metal plate platform for stabilization and easy transportation. The entire system can be placed on a cart and is easily transported for outdoor image acquisition. The mirror is mounted on a geared spinning mechanism, which is powered by a 12 V DC motor. The spinning speed can be adjusted by changing the gear ratio. The aspect ratio of acquired images can be changed by adjusting the gear ratio along with camera exposure time.

The bellows connects to the camera and the lens at two ends. The bellows length is adjustable for changing the focus and magnification. For long-range inspection applications, our goal is to image an area of interest in a remote scene with a hyper-resolution of 6,144 pixels in one dimension. This differs from the close-range imaging system, since the scene is far away from the camera; in order to form an image of the scene on the camera sensor plane, a long focal-length lens and a relatively short bellows length (∼20 cm) should be used. Figure 10b illustrates the optical path of

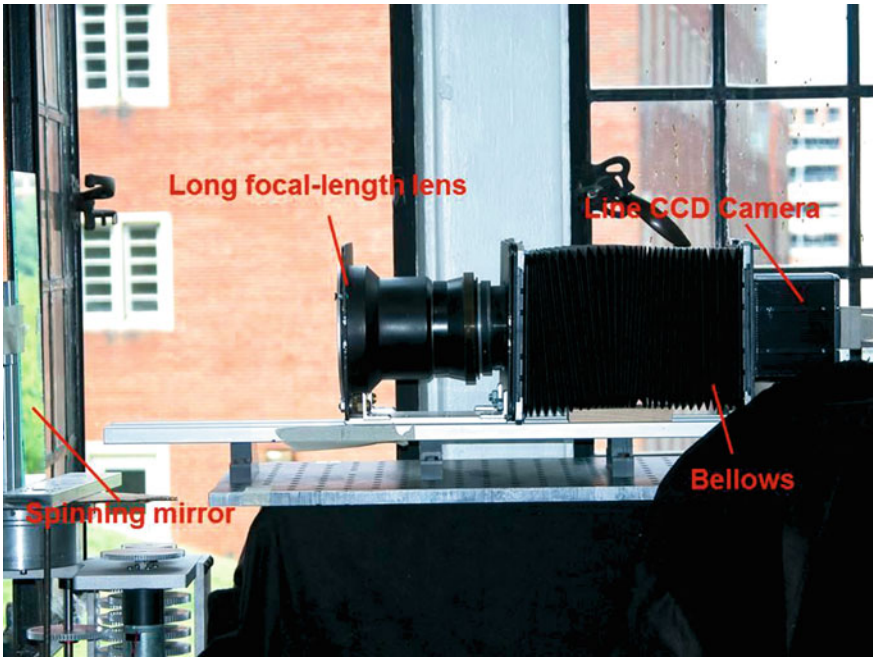

Fig. 11 Long-range imaging system

image formation for long-range imaging. The distances between the object and lens, the lens and image are also related by the thin lens formula, given by Eq.1.

3 Color Misalignment Correction

The hyper-resolution images acquired by both multi-line CCD imaging systems mentioned in the previous section intrinsically have a color misalignment defect, which must be fixed before the images can be useful. In this section, we present a technique to automatically correct this defect.

3.1 Formulations of Color Misalignment

Color misalignment in multi-line CCD imaging is measured by the number of pixels and is determined by the relative scan motion between the camera and the object, the optical parameters, the imaging parameters, and the physical distance between adjacent color sensor lines. The pixel displacement between images acquired by different CCD channels is directly related to the CCD line rate (approximately the inverse of exposure time). For example, assume that we are taking images of a tiny point. The point is so small that its image can fall on only one color sensor line at one time. The amount of time that takes the point image to travel from one color sensor line to the next is determined by the relative motion between the camera and the point object, the optical parameters (distances, focus, etc.), and the physical distance between adjacent color channels. During this period of time, the line acquisition rate or the number of exposures of this color channel will determine the number of pixels between the two point images on adjacent color planes in the resulting image.

Figure 12 illustrates the factors that determine color misalignment in multi-line CCD images acquired by the translational scan scheme, and Fig. 13 illustrates the factors for the rotational scan scheme. The primary factors determining color misalignment include:

(1) τ, time that a point image in the image plane traverses from one color channel to the next;
(2) R, CCD sensor line scan rate or the inverse of exposure time.

The pixel displacement in color misalignment, D, can be formulated as

$$D = R\tau. \tag{2}$$

The point image traverse time, τ, can be determined by secondary factors which include:

(1) d_o, distance from the object plane to the center of camera lens;

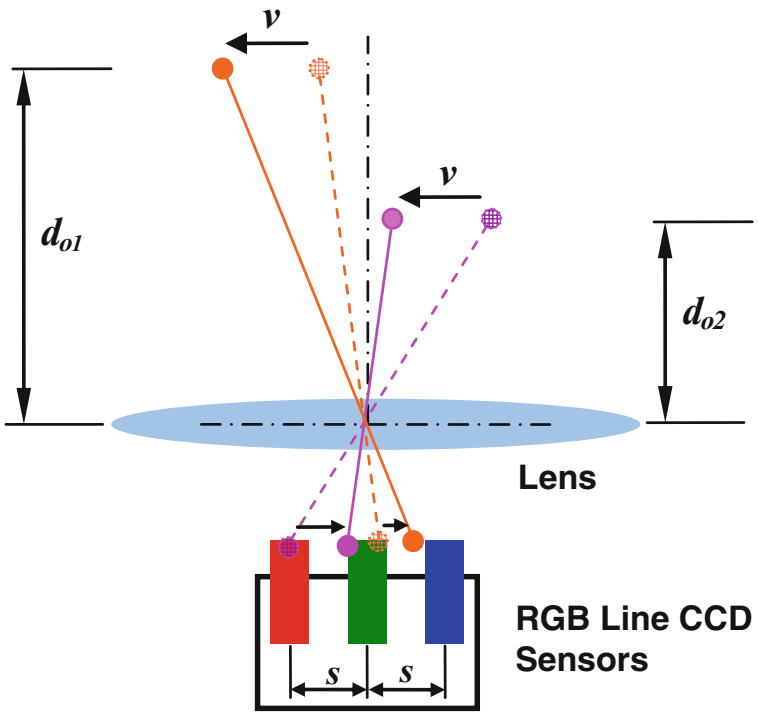

Fig. 12 Factors that affect color misalignment in multi-line CCD images acquired by a translational scan scheme

(2) v, relative motion speed between the object and the line CCD camera;
(3) f, focal length of the camera lens;
(4) s, color channel separation.

In a translational scan scheme, the time τ that takes a point image to travel from one color channel to the next can be formulated as follows,

$$\tau = \frac{d_i v}{d_o s}, \tag{3}$$

where d_o is the distance from the object plane to the center of the lens, d_i is the distance from the image plane to the center of the lens, v is the translational motion speed of the object, and s is the separation distance between the centers of adjacent color sensor lines. It can be derived from Eq. 1 that

$$d_i = \frac{d_o f}{d_o - f}. \tag{4}$$

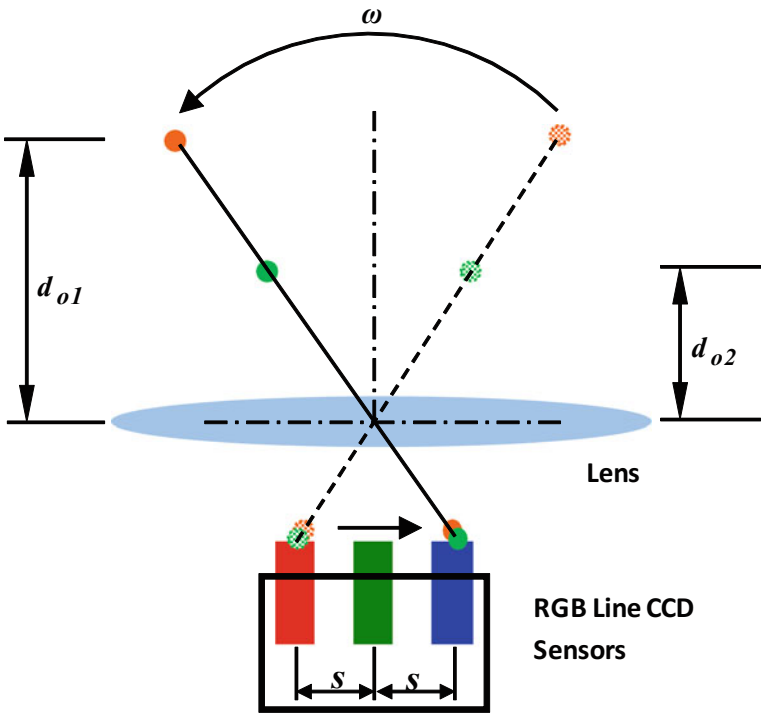

Fig. 13 Factors that affect color misalignment in multi-line CCD images acquired by rotational scan scheme

After substituting Eqs. 3 and 4 into Eq. 2, we obtain a new formulation of color misalignment which can be easily calculated from camera and imaging parameters as follows,

$$D_T = \frac{f v R}{(d_o - f)s}. \tag{5}$$

By examining Eq.5, one can conclude that the pixel displacement in color misalignment is the same everywhere for an entire image acquired by the close-range imaging system with a translational scan scheme, because the object to be imaged in such scenario is usually a surface or an object with a shallow depth that is much smaller than d_o. Therefore, the distance between the object surface and the camera lens, d_o, is the same for the entire surface when imaging is taking place, so the color misalignment is also the same for different parts of the image.

Similarly, in a rotational scan scheme, the time τ that takes a point image to travel from one color channel to the next can be formulated as follows,

$$\tau = \frac{\omega d_i}{s}, \tag{6}$$

where ω is the angular speed of the rotational scan motion. Substituting Eqs. 4 and 6 into Eq. 2, we obtain a formulation of color misalignment in long-range multi-line CCD images acquired with a rotational scan scheme as

$$D_R = \frac{f\omega d_o R}{(d_o - f)s}. \tag{7}$$

It can be noted, that for a long-range imaging system the object distance is much larger than the focal length of the camera lens, and Eq. 7 can be approximated as

$$D_R \approx f\omega R/s, \text{ for } d_o >> f. \tag{8}$$

Equation 8 indicates that color misalignment in long-range multi-line CCD images is independent of the object distance; therefore, different objects of different distances from the camera in a scene would have the same color misalignment in the same image. An experiment was conducted to test the validity of Eq. 8. Figure 14 shows a long-range multi-line CCD image, and the color misalignment values for objects of different distances in the image are listed in Table 1. It can be seen that those objects of different distances from the camera have exactly the same pixel displacement, and the observation results agree well with the above theoretical analysis.

Therefore, we can conclude that the pixel displacement in color misalignment is the same for an entire image in almost all circumstances for the two types of multi-line CCD imaging systems that we developed. This makes the task a lot easier to develop an algorithm to fully automatically and accurately detect and correct the color misalignment in acquired multi-line CCD images.

3.2 Correction of Color Misalignment

Since the pixel displacement in color misalignment is the same for an entire image, in order to automatically correct this misalignment in multi-line CCD images we must develop a method to automatically detect the amount of displacement and use this value to shift the R, G, B color planes to correct the color misalignment. This method is applied after the image acquisition process is completed, thereby putting

Fig. 14 Test image for studying the relationship between object distance and color misalignment

Table 1 Color misalignment for objects of different distances from the camera

Patch #	Object distance (m)	Color misalignment (pixels)
1	5	8
2	15	8
3	20	8
4	900	8
5	1200	8
6	1300	8
7	1500	8
8	1600	8

no constraints on imaging parameters. In this way, desired imaging parameters can be used to obtain images with desirable aspect ratio, brightness, contrast, etc. An algorithm developed to automatically correct color misalignment in multi-line CCD images is described as follows:

1. Slice the multi-line-scan RGB image into three color planes – R, G, B.
2. Calculate an estimate of the pixel displacement of color misalignment, D, according to Eqs. 5 or 8. Then shift the R-plane and B-plane, with all possible displacements in the scan direction within a specified range $[-(1+\delta)D, -(1-\delta)D]$ or $[(1-\delta)D, (1+\delta)D]$, in the anticipated direction of color misalignment, where δ is a threshold chosen by user. The shift tends to realign the R-plane and B-plane with the G-plane.
3. For each displacement, calculate the gray-level distances between adjacent color planes for all displacements with the following formula

$$\begin{cases} D_{RG}(d_R) = \sqrt{\sum_{x,y} (I_R(d_R, x, y) - I_G(x, y))^2} \\ D_{GB}(d_B) = \sqrt{\sum_{x,y} (I_G(d_B, x, y) - I_B(x, y))^2} \end{cases} \quad (9)$$
$$\forall d_R, d_B \in [-(1+\delta)D, -(1-\delta)D] \text{ or } [(1-\delta)D, (1+\delta)D]$$

   where $I_*(x, y)$ is an original color-plane image, $I_*(d_*, x, y)$ is a color-plane image shifted with a displacement of d_*, $*$ represents R or B, and x, y are pixel coordinates.
4. Find the minimum $D_{RG}(d_R)$ and $D_{GB}(d_B)$. The corresponding displacements, d_{R-Opt} and d_{B-Opt}, are the correct color misalignment in the corresponding image.
5. Correct the color misalignment in the image by shifting the R-, B-plane by the corresponding detected pixel displacement, d_{R-Opt} and d_{B-Opt}, and superimpose them with the G-plane to reconstruct the color-misalignment-corrected image.

In Step 3 of the above procedure, instead of using gray-level distances between adjacent color planes as a criterion, other criteria can be applied, e.g., cross correlation of adjacent color channels. If cross correlation is used in Step 4, the correct

pixel displacement in color misalignment corresponds to the maximum cross correlation.Based on extensive tests, we found that cross correlation gives the same results as the gray-level distance between color planes. It is also worth noting that, in Step 2, the pixel displacement of the color misalignment does not have to be estimated according to Eqs. 5 or 8 as long as the search range of the pixel displacement is sufficiently large. However, a larger search range might significantly increase the processing time, given the hyper-resolution of multi-line CCD images. Figure 15 illustrates the proposed method of color misalignment correction

4 Experimental Results

The multi-line CCD camera used in our imaging systems is a high-performance PerkinElmer YD5060 tri-linear digital line-scan color camera. The output speeds are up to 90 MHz (30 MHz per output, each output corresponding to either the red, green, or blue color channel), pixel resolution of 6,144, and line scan rates up to 4.88 kHz. The camera features a geometrically precise photodiode CCD image sensor, with 10 μm square photo-elements. Line spacing between the color-filtered linear rows is 40 μm [24].

Color separation and imaging are accomplished through the tri-linear image sensor in the YD5060. However, given the 40 μm center-to-center spacing between the color lines, the image must be reconstructed to correct color misalignment and combine the colors into a usable image. The YD5060 provides a functionality that allows the user to set a delay in the camera, so as to synchronize the camera to its target. Delay can be set from + 15 to –15 lines, allowing the camera to image in either direction,

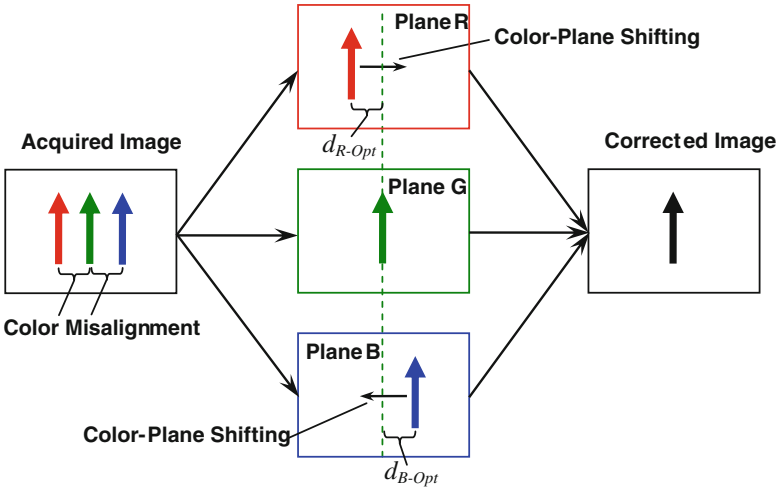

Fig. 15 Illustration of color misalignment correction